

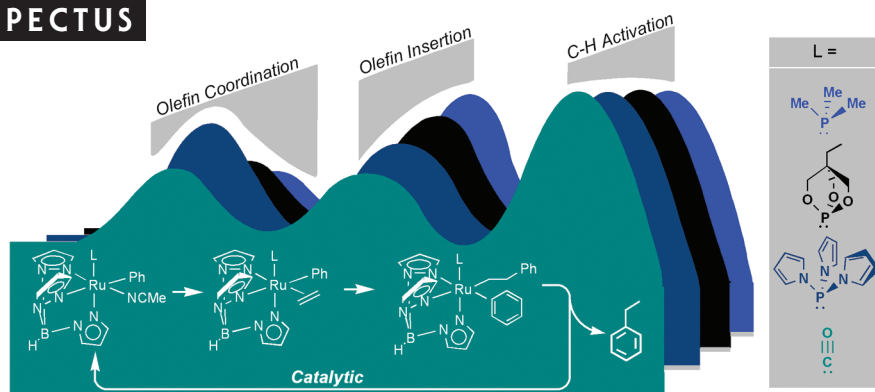
## Ru(II) Catalysts Supported by Hydridotris(pyrazolyl)borate for the Hydroarylation of Olefins: Reaction Scope, Mechanistic Studies, and Guides for the Development of Improved Catalysts

NICHOLAS A. FOLEY,<sup>†</sup> JOHN P. LEE,<sup>†</sup> ZHUOFENG KE,<sup>§</sup>  
T. BRENT GUNNOE,<sup>†,\*</sup> AND THOMAS R. CUNDARI<sup>§,\*</sup>

<sup>†</sup>Department of Chemistry, University of Virginia, Charlottesville, Virginia 22904-4319, <sup>§</sup>Center for Advanced Scientific Computing and Modeling (CASCaM), Department of Chemistry, University of North Texas, Box 305070, Denton, Texas 76203-5070

RECEIVED ON AUGUST 28, 2008

### CON SPECTUS



Carbon–carbon bond formation is the central method by which synthetic chemists add complexity, which often represents value, to molecules. Uniting a carbon chain with an aromatic substrate to yield an alkyl arene product is thus a molecular means of creating value-added materials. A traditional method for generating alkyl arenes is Friedel–Crafts catalysis, in which an alkyl halide or olefin is activated to react with an aromatic substrate. Unfortunately, despite the development of new generations of solid-state catalysts, the reaction often requires relatively harsh conditions and frequently gives poor to moderate selectivity. Conversely, a halide can first be incorporated into the aromatic ring, and the aryl halide can subsequently be joined by a variety of catalytic coupling techniques. But generating the aryl halide itself can be problematic, and such methods typically are not atom-economical. The addition of aromatic C–H bonds across the C–C double bonds of olefins (olefin hydroarylation) is therefore an attractive alternative in the preparation of alkyl arenes.

Despite the dominance and practical advantages of heterogeneous catalysts in industrial synthesis, homogeneous systems can offer an enhanced ability to fine-tune catalyst activity. As such, well-defined homogeneous catalysts for the hydroarylation of olefins provide a potentially promising avenue to address issues of selectivity, including the production of monoalkylated arene products and the control of linear-to-branched ratios for synthesis of long-chain alkyl arenes, and provide access to more ambient reaction conditions. However, examples of homogeneous catalysts that are active for the conversion of unactivated aromatic and olefin substrates to alkyl arene products that function via metal-mediated C–H activation pathways are limited. In this Account, we present results from research aimed at the development of Ru(II) catalysts supported by the hydridotris(pyrazolyl)borate (Tp) ligand for the addition of aromatic C–H bonds across olefins. On the basis of detailed mechanistic studies with  $\text{TpRu(L)(NCMe)R}$  catalysts, in which the neutral ancillary ligand L is varied, we have arrived at guidelines for the development of improved catalysts that are based on the octahedral- $d^6$  motif.

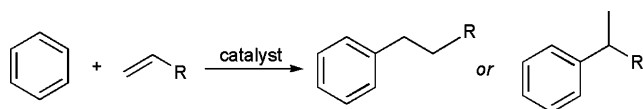
## 1. Introduction

Since initial reports of selective metal-mediated C–H activation, substantial understanding of these transformations has been achieved,<sup>1,2</sup> and useful catalysts for C–H bond functionalization are emerging.<sup>3–5</sup> Such reactions offer the possibility of more efficient conversion of hydrocarbons into higher value materials. For example, olefin hydroarylation is an atom-economical route for construction of C–C bonds involving aromatic substrates (Scheme 1). Most commonly, alkylarene synthesis has been accomplished via Friedel–Crafts catalysis;<sup>6</sup> however, such reactions have limitations.<sup>6,7</sup> For example, due to the mechanism, linear alkyl chains cannot be accessed, and products are often more reactive than starting materials leading to polyalkylation. New zeolite technologies have provided increased selectivity for monoalkylated products with reduced waste.<sup>8</sup> Yet they require unique structural design for each alkylarene synthesis and cannot select for linear alkylbenzenes, and polyalkylation is still problematic for some systems.<sup>9</sup>

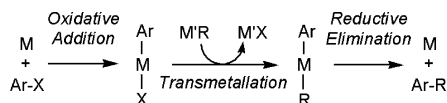
Catalytic Suzuki, Heck, Sonogashira, Stille, Negishi, and related reactions provide useful methods for C–C bond formation involving aromatic substrates (Scheme 2).<sup>10,11</sup> However, such reactions require the incorporation of halide into the aromatic substrate, which is often a low yield process that generates halogen-containing waste. Furthermore, with the exception of the Heck reaction, these catalysts generate a stoichiometric quantity of metal-containing waste.

Catalytic olefin hydroarylation via a pathway involving olefin insertion and metal-mediated aromatic C–H activation can, in principle, overcome the aforementioned limitations. However, avoiding side reactions whose energy profiles are often similar to desired transformations is challenging (Scheme 3). Competition can arise from irreversible  $\beta$ -hydride elimination, irreversible C–H oxidative addition, C–H activation of substrates other than the arene, and multiple olefin insertions. Thus, an efficient catalyst must provide kinetic access to insertion of a single olefin equivalent and selectively activate arene

**SCHEME 1.** Hydroarylation of Olefins



**SCHEME 2.** Transition Metal-Catalyzed Aryl–Carbon Coupling Involves Carbon–Halide Activation and Transmetalation



**SCHEME 3.** Metal-Catalyzed Olefin Hydroarylation (Red) and Common Side Reactions

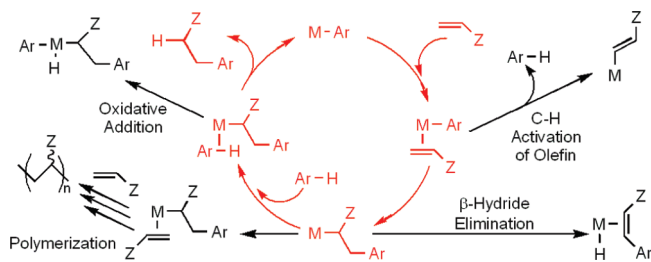
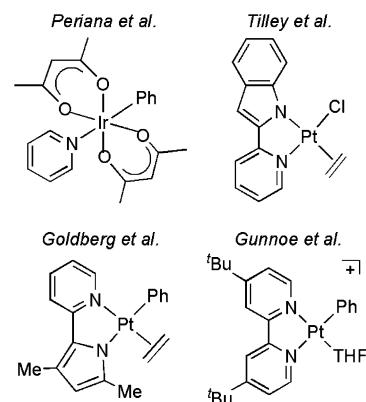


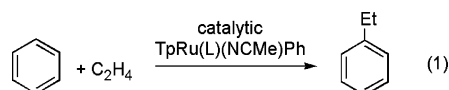
**CHART 1.** Transition Metal Catalysts for Olefin Hydroarylation

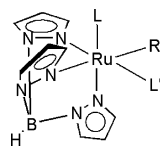


matic versus olefin C–H bonds. These demands result in a narrow window for success.

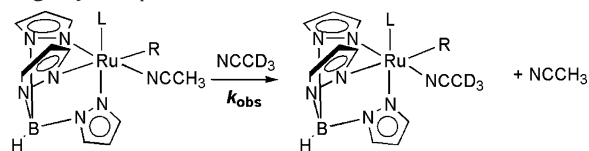
In addition to the Ru(II) systems discussed herein, a few catalysts for olefin hydroarylation with unactivated substrates have been reported (Chart 1). Interestingly, Pt(II) catalysts for olefin hydroarylation with mild selectivity for *n*-alkylbenzenes as well as selectivity for branched products have been reported.<sup>12–14</sup> An Ir(III) catalyst is robust, and this system shares many mechanistic features with the Ru systems discussed herein.<sup>15</sup>

We have been investigating Ru(II) catalysts of the type  $\text{TpRu(L)(NCMe)R}$  {Tp = hydridotris(pyrazolyl)borate; L = CO,  $\text{PMe}_3$ ,  $\text{P(pyr)}_3$ , or  $\text{P(OCH}_2)_3\text{CEt}$ ; R = hydrocarbyl; pyr = *N*-pyrrolyl} for olefin hydroarylation (eq 1).<sup>7,16–26</sup> Despite the potential impact of catalytic olefin hydroarylation and recent advances,<sup>27,28</sup> opportunities to study structure/activity relationships have been rare. We felt that  $\text{TpRu(L)R}$  fragments would be ideal for detailed studies through modification of L, which permits incremental adjustment of metal electron density and steric profile.



**CHART 2.** Structure of TpRu(L)(L')R (Table 1 lists L, R, and L')**TABLE 1.** TpRu(L)(L')R systems.

complex	L	R	L'
1	CO	Me	NCMe
2	CO	Ph	NCMe
3	PMe <sub>3</sub>	Me	NCMe
4	PMe <sub>3</sub>	Ph	NCMe
5	P(pyr) <sub>3</sub> <sup>a</sup>	Me	NCMe
6	P(pyr) <sub>3</sub> <sup>a</sup>	Ph	NCMe
7	κ <sup>2</sup> -P,C-P(pyr) <sub>2</sub> (NC <sub>4</sub> H <sub>3</sub> ) <sup>a</sup>	κ <sup>2</sup> -P,C-P(pyr) <sub>2</sub> (NC <sub>4</sub> H <sub>3</sub> ) <sup>a</sup>	NCMe
8	P(OCH <sub>2</sub> ) <sub>3</sub> CeT	Ph	NCMe
9	CO	2-furyl	NCMe
10	CO	2-thienyl	NCMe
11	PMe <sub>3</sub>	η <sup>3</sup> -C <sub>3</sub> H <sub>4</sub> Me	
12	PMe <sub>3</sub>	Ph	η <sup>2</sup> -C <sub>2</sub> H <sub>4</sub>
13	PMe <sub>3</sub>	η <sup>1</sup> -C <sub>2</sub> H <sub>3</sub>	η <sup>2</sup> -C <sub>2</sub> H <sub>4</sub>
14	PMe <sub>3</sub>	CH <sub>2</sub> CH <sub>2</sub> CH=CH	η <sup>2</sup> -C <sub>2</sub> H <sub>4</sub>
15	PMe <sub>3</sub>	η <sup>1</sup> -C <sub>2</sub> H <sub>3</sub>	NCMe
16	CO	η <sup>3</sup> -C <sub>3</sub> H <sub>4</sub> Me	

<sup>a</sup> pyr = *N*-pyrrolyl.**TABLE 2.** Experimental *k*<sub>obs</sub> and Δ*G*<sup>‡</sup>s for Degenerate NCMe/NCCD<sub>3</sub> Exchange by Complexes **2**, **4**, and **5**.L = CO (**2**), PMe<sub>3</sub> (**4**) or P(pyr)<sub>3</sub> (**5**); R = Me or Ph

complex	temp (°C)	<i>k</i> <sub>obs</sub> (×10 <sup>-4</sup> s <sup>-1</sup> )	relative to <i>k</i> <sub>obs</sub> of <b>2</b>	Δ <i>G</i> <sup>‡</sup> (kcal/mol)
<b>2</b>	70	0.32(2)	1	27.2(1)
<b>4</b>	60	1.56(4)	4.9	25.4(1)
<b>5</b>	60	1.47(2)	4.6	25.4(1)

## 2. Catalyst Architecture

Complexes discussed here possess the formally anionic 6e<sup>-</sup> donor (κ<sup>3</sup>-coordination) Tp, a 2e<sup>-</sup> donor neutral ancillary ligand (L), NCMe or η<sup>2</sup>-C<sub>2</sub>H<sub>4</sub> (L'), and hydrocarbyl (R) ligand (Chart 2 and Table 1). For all TpRu(L)(NCMe)R systems, NCMe is sufficiently labile at moderate temperatures to provide five-coordinate TpRu(L)R systems that are necessary to bind and activate olefin or aromatic substrates. Since degenerate NCMe/NCCD<sub>3</sub> exchange from TpRu(L)(NCCH<sub>3</sub>)R in NCCD<sub>3</sub> is proposed to be dissociative,<sup>7,22,23</sup> the Δ*G*<sup>‡</sup> for exchange of isotopomers should depend upon the rate of NCMe dissociation for **2**, **4**, and **5** (Table 2). Although data are limited, the relative rates of NCMe dissociation from TpRu(L)(NCMe)Ph complexes correlate with the donating ability of L.

The ancillary ligand L has been varied among CO,<sup>29</sup> P(pyr)<sub>3</sub>,<sup>30</sup> P(OCH<sub>2</sub>)<sub>3</sub>CeT,<sup>29,31</sup> and PMe<sub>3</sub>,<sup>29</sup> which provides a

**TABLE 3.** Comparison of Cone Angle and Ru(III/II) Redox Potentials for Ligands upon Coordination to {TpRu(NCMe)Ph}

Ligand:					
<b>Electronic Effect:</b> Ru(III/II) Ox. potential of TpRu(L)(NCMe)Ph (V) (vs. NHE)	1.03	0.82	0.55	0.29	
<b>Steric Perturbation:</b> Cone Angle (°)	95 <sup>a</sup>	145 <sup>b</sup>	101 <sup>a</sup>	118 <sup>a</sup>	

<sup>a</sup> Reference 29. <sup>b</sup> Reference 30.

means of tuning the sterics and electronics of TpRu(L)(NCMe)R (Table 3). We have used reversible Ru(III/II) potentials obtained from cyclic voltammetry to estimate the relative electron density among catalyst precursors and thus determine the impact of metal electron density, as a function of L, on catalysis. The relative electron densities of the Ru phenyl complexes are **4** (PMe<sub>3</sub>) > **8** {P(OCH<sub>2</sub>)<sub>3</sub>CeT} > **6** {P(pyr)<sub>3</sub>} > **2** (CO).

## 3. Stoichiometric Aromatic C–H Activation by TpRu(L)(NCMe)R as a Function of L

Catalytic hydrophenylation of ethylene by TpRu(CO)(NCMe)Ph reveals an intermolecular kinetic isotope effect (C–H activation of C<sub>6</sub>H<sub>6</sub> vs C<sub>6</sub>D<sub>6</sub>) of *k*<sub>H</sub>/*k*<sub>D</sub> = 2.1(1),<sup>7</sup> suggesting that benzene C–H activation is rate-determining. Therefore, decreasing the activation barrier to aromatic C–H activation should enhance catalyst activity, and thus, we sought to understand the impact of L on this transformation.

The complexes TpRu(L)(NCMe)R mediate stoichiometric C–H activation of aromatic substrates to generate TpRu(L)-(NCMe)Ar and RH (eqs 2–4).<sup>7,16,17,22</sup> Benzene activation upon reaction of TpRu(L)(NCMe)Ph and C<sub>6</sub>D<sub>6</sub> have been traced by <sup>1</sup>H/<sup>2</sup>H NMR spectroscopy (eq 4),<sup>22,26</sup> and mechanistic studies indicate that the pathway in Scheme 4 is most likely.<sup>7,22</sup> Acetonitrile dissociation creates a vacant site for reversible benzene coordination, which precedes *rate-determining* C–H activation and subsequent coordination of acetonitrile to form TpRu(L)(NCMe)Ph. Consistent with the proposed pathway, increasing the concentration of free acetonitrile suppresses the rate of C<sub>6</sub>D<sub>6</sub> C–D activation.<sup>7,16,22</sup> Strongly bound isonitrile ligands retard benzene C–H(D) activation (eq 6),<sup>22</sup> which provides additional evidence that 16-electron TpRu(L)R systems are responsible for aromatic C–H activation. Similar to catalytic reactions, kinetic isotope effects are observed for benzene activation by TpRu(L)(NCMe)Me (L = CO or PMe<sub>3</sub>; eq 5).<sup>7,22</sup> DFT calculations (see below) indicate that the transition state for benzene C–H bond breaking is the highest

energy species on the reaction coordinate for overall benzene C–H activation.

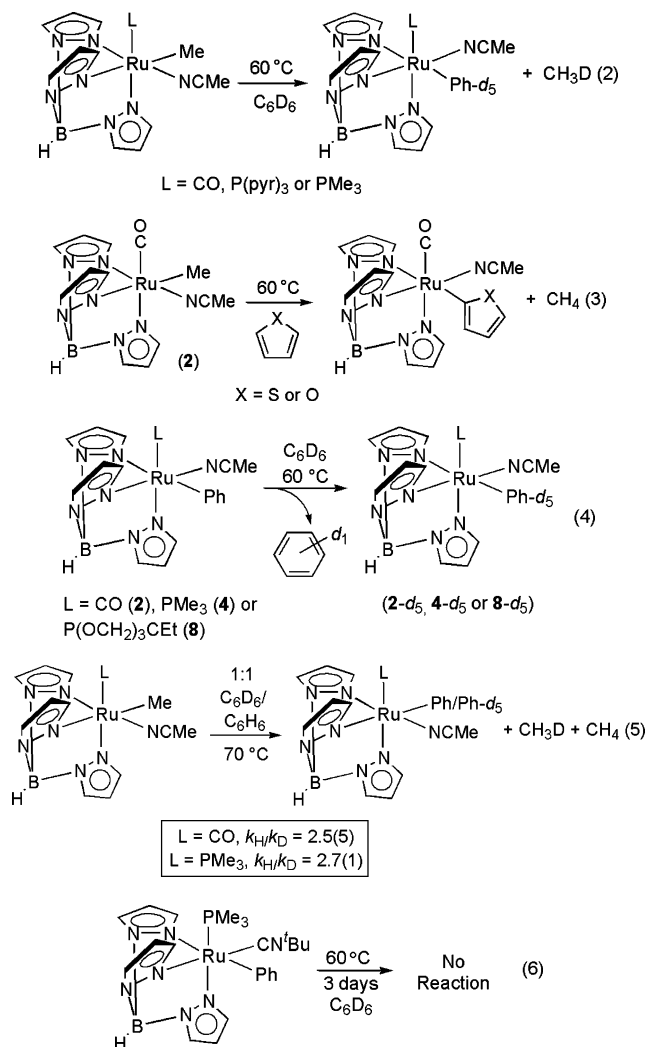
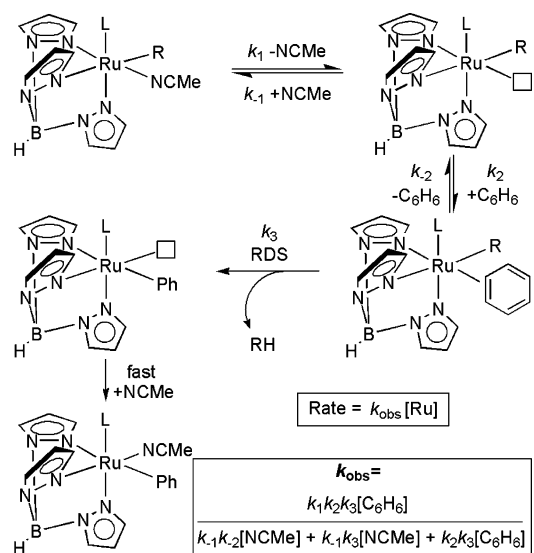


Table 4 displays  $k_{\text{obs}}$  values for C<sub>6</sub>D<sub>6</sub> activation by CO complex **2**, PMe<sub>3</sub> complex **4**, and phosphite complex **8** in the presence of 1 equiv of acetonitrile (0.035 M). Analysis of benzene C–H(D) activation by P(pyr)<sub>3</sub> complexes **5** and **6** is complicated by yields that are <70%.<sup>23</sup> A plot of  $k_{\text{obs}}$  for C<sub>6</sub>D<sub>6</sub> activation versus Ru(III/II) potential gives a linear correlation with  $R^2 = 0.97$  (Figure 1). Despite limited data and multiple factors that may contribute to  $k_{\text{obs}}$  for benzene C–H activation (Scheme 4), this trend indicates that increased metal electron density facilitates the overall rate of benzene C–H activation.<sup>32</sup> Furthermore, the relationship suggests that  $d^6/d^5$  redox potentials might be viable predictors of activity for TpRu(L)(NCMe)R catalysts, related Ru(II) systems and other  $d^6$  complexes.

Computational studies utilizing the B3LYP hybrid functional and effective core potentials indicate that  $\Delta G^\circ$  for benzene coordination is largely dependent on the steric profile of L (Scheme 5; Figure 2). For example, PEt<sub>3</sub> and PMe<sub>3</sub> are

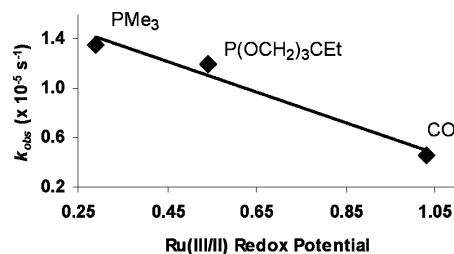
**SCHEME 4.** Proposed Pathway and Rate Law for Benzene C–H Activation by TpRu(L)(NCMe)R [ $[Ru]$  = Concentration of TpRu(L)(NCMe)R]



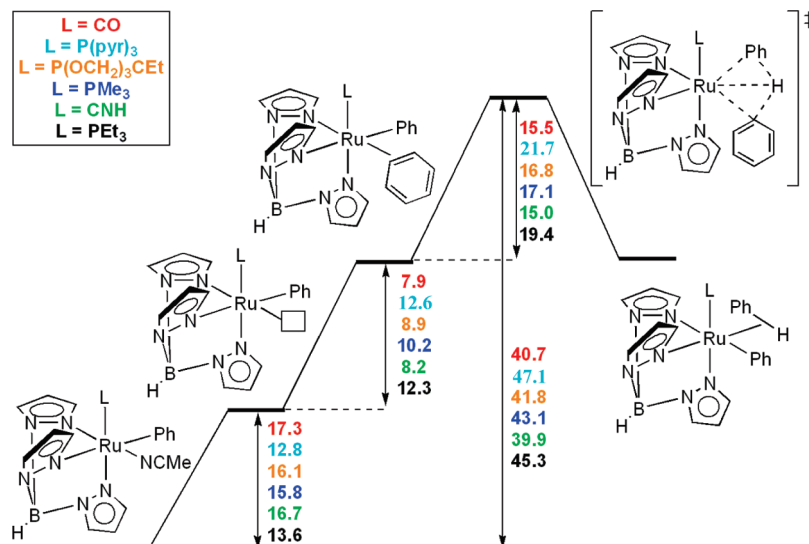
**TABLE 4.** Rate Constants for Benzene C–H(D) Activation by TpRu(L)(NCMe)Ph at 60 °C with Added NCMe (0.035 M)

complex	$k_{\text{obs}} (\times 10^{-5} \text{ s}^{-1})$	$\Delta G^\ddagger$ (kcal/mol)
<b>4</b>	1.36(4)	27.0(5)
<b>8</b>	1.20(2)	27.1(1)
<b>2</b>	0.462(3)	27.7(1)

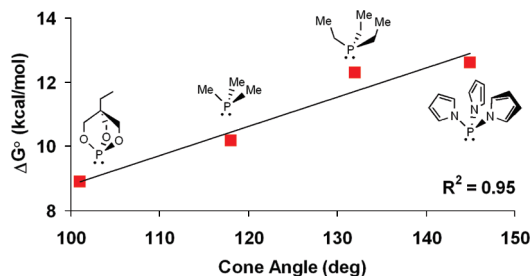
expected to differ little in terms of  $\sigma$ -donating ability, and the 2.1 kcal/mol difference in binding free energy of benzene to TpRu(L)Ph is ascribed to the difference in steric bulk (cone angles: PMe<sub>3</sub> = 118°; PEt<sub>3</sub> = 132°).<sup>29</sup> The calculated dependence of benzene coordination on steric profile of L (i.e., larger L inhibits benzene coordination) suggests that complexes with bulky phosphines might be less proficient at aromatic C–H activation, consistent with experimental studies of P(pyr)<sub>3</sub> complexes **5** and **6**.<sup>23</sup> Heating the methyl complex **5** in benzene does produce methane and the phenyl complex **6**; however, the yield (<sup>1</sup>H NMR) of **6** is <70% under all conditions studied (eq 7). Likewise, heating **6** in C<sub>6</sub>D<sub>6</sub> produces C<sub>6</sub>H<sub>5</sub>D and **6-d**<sub>5</sub> but again with yields < 70% (eq 8). The low yields for benzene C–D activation likely reflect the difficulty in substituting the linear NCMe ligand with the more sterically imposing



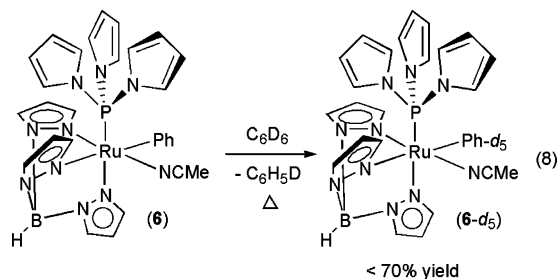
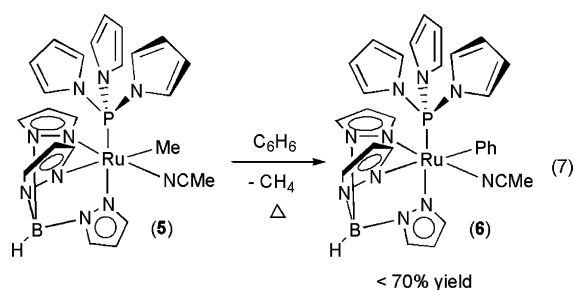
**FIGURE 1.** Plot of Ru(III/II) potentials versus  $k_{\text{obs}}$  for C<sub>6</sub>D<sub>6</sub> C–H activation by TpRu(L)(NCMe)Ph.  $R^2 = 0.97$ .

**SCHEME 5.** Calculated Free Energy (kcal/mol; 298 K) for Benzene C–H Activation by TpRu(L)(NCMe)Ph<sup>a</sup>

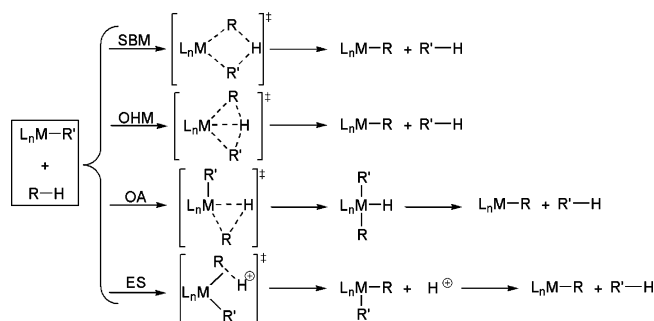
<sup>a</sup> Benzene adduct is shown as  $\eta^2$ -C,C, although in some cases  $\eta^2$ -C,H is the calculated coordination mode.

**FIGURE 2.** Plot of ligand cone angle versus calculated  $\Delta G^\circ$  (kcal/mol, 298 K) for benzene coordination to TpRu(L)Ph.

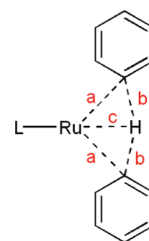
benzene to TpRu{P(pyr)<sub>3</sub>}<sub>3</sub>(R), which allows decomposition pathways to compete with benzene C–H activation.



The mechanism of C–H activation determines the influence of ligand parameters on the propensity toward C–H

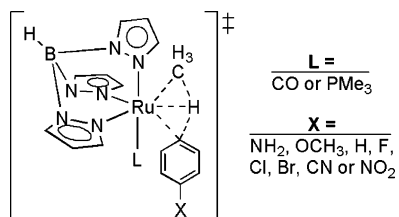
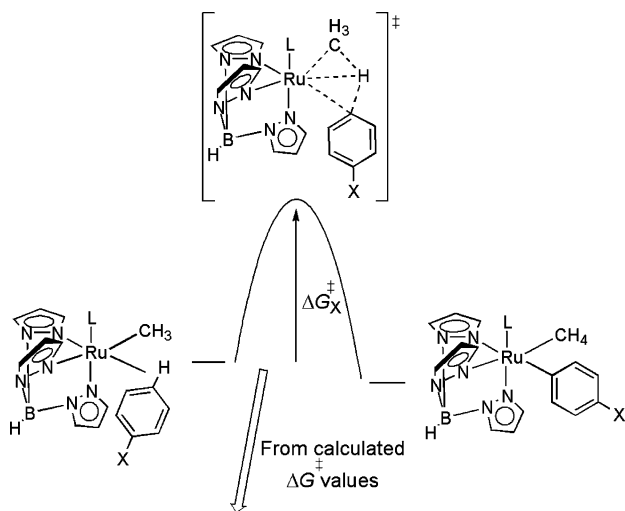
**SCHEME 6.** Mechanisms for C–H Activation:  $\sigma$ -Bond Metathesis (SBM), Oxidative Hydrogen Migration (OHM), Oxidative Addition (OA), and Electrophilic Substitution (ES)

bond cleavage, and several pathways for C–H activation have been elucidated for metal-mediated C–H activation (Scheme 6).<sup>1</sup> Computational and experimental studies of C–H activation by TpRu(L)R on model Tab–Ru {Tab = tris(azo)borate} and full Tp–Ru models suggest that the transformations traverse concerted  $\sigma$ -bond metathesis (SBM) pathways with close Ru–H contacts.<sup>7,17,33,34</sup> Figure 3 and Table 5 contain calculated bond distances in benzene C–H activation transition states for TpRu(L)(C<sub>6</sub>H<sub>6</sub>)Ph {L = CO, P(pyr)<sub>3</sub>, P(OCH<sub>2</sub>)<sub>3</sub>Ct, and PMe<sub>3</sub>} with

**FIGURE 3.** Transition state geometry for benzene C–H activation by TpRu(L)(C<sub>6</sub>H<sub>6</sub>)Ph (see Table 5 for calculated distances *a*, *b*, and *c*; note, relative orientation of phenyl rings and Ru/H not depicted).

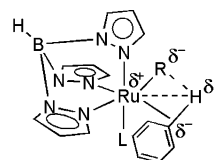
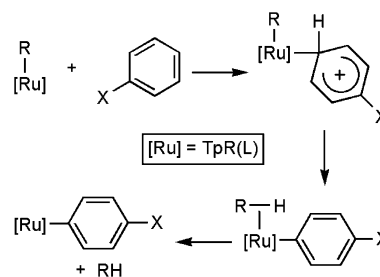
**TABLE 5.** Calculated Distances (Å) for C–H Activation Transition State of TpRu(L)(C<sub>6</sub>H<sub>6</sub>)Ph

L	Ru–C (a)	Ru–H (b)	C–H (c)
CO	2.19	1.65	1.61
P(pyr) <sub>3</sub>	2.21	1.64	1.57/1.60
P(OCH <sub>2</sub> ) <sub>3</sub> CEt	2.18	1.61	1.69
PMe <sub>3</sub>	2.18	1.61	1.66

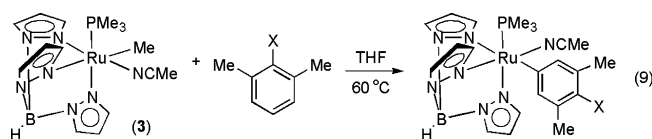
**CHART 3.** TpRu(L)Me Complexes and *para*-Substituted Arenes to Probe Mechanism of C–H Activation**SCHEME 7.** Computational Studies of C–H Activation by TpRu(L)(Me)(C<sub>6</sub>H<sub>5</sub>X) Give Hammett Plots (versus  $\sigma_p$ ) with Good Linear Fits (X = NO<sub>2</sub>, CN, Br, Cl, F, H, OMe, and NH<sub>2</sub>)

Plot  $k_X/k_H$  versus Hammett  $\sigma_p$  parameters gives linear fit with  $\rho = 2.6$  (L = CO) and 3.2 (L = PMe<sub>3</sub>)

Ru–H contacts ranging from 1.61 to 1.65 Å (Table 5). Calculations suggest that increasing the donor ability of L results in shorter Ru–H distances in the transition state, consistent with enhanced Ru-to-H electron donation as the donor ability of L is increased. More extensive C–H bond breaking results in shorter M–C and M–H bond distances. Thus, computational studies of aromatic C–H activation by TpRu(L)R suggest a SBM-type transition state bearing protic character on the activated hydrogen. To compensate for this protic character, the metal back-donates electron density from a filled orbital to the transannular hydrogen, which has been termed oxidative hydrogen migration (OHM) and is thus differentiated from SBM with d<sup>0</sup> metal centers.<sup>35,36</sup> The formal oxidation state of Ru in the transition state is perhaps best considered as Ru(IV).

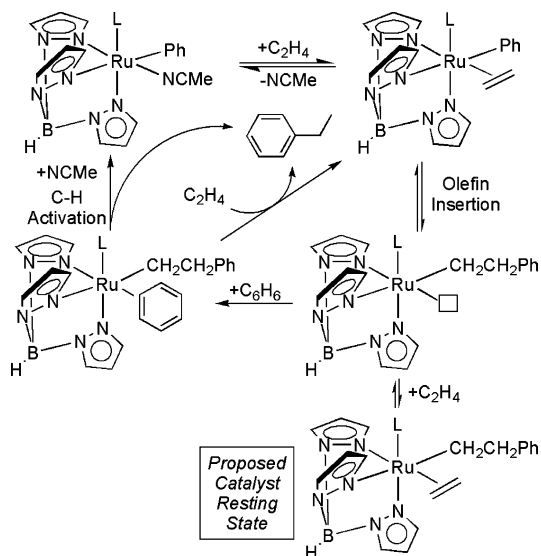
**SCHEME 8.** Model of Transition State for C–H Activation of Benzene by TpRu(L)R**SCHEME 9.** Wheland-Type Intermediate in Electrophilic Aromatic Substitution ([Ru] = TpRu(L)) Is Not the Operative Mechanism for TpRu(L)R Systems

To further probe C–H activation, an experimental/computational Hammett study of aromatic C–H activation by TpRu(L)Me (L = CO or PMe<sub>3</sub>) (Chart 3) was performed.<sup>32</sup> Experimentally, for the xylol compounds, aromatic C–H activation is only observed when X is electron-withdrawing (eq 9). Calculations of C–H activation from the arene adducts TpRu(L)(Me)(C<sub>6</sub>H<sub>5</sub>X) (X is *para* to the activated hydrogen) reveal good linear fits in Hammett plots with positive slopes (Scheme 7). These studies are consistent with Ru coordination of the aromatic C–H bond, which results in negative charge localized into the aromatic ring (Scheme 8), followed by transfer of a proton via SBM. Stated succinctly, the metal coordinates the aromatic C–H bond and activates it toward a “metal-assisted” intramolecular proton transfer to a basic hydrocarbyl ligand (Scheme 8). Notably, the Hammett studies provide evidence against an electrophilic aromatic substitution pathway (Scheme 9).



For X = H, NH<sub>2</sub>, OMe: decomposition  
For X = NO<sub>2</sub>: 33% isolated yield, 48% yield by NMR  
For X = Br: 23% isolated yield, 33% yield by NMR

Calculated  $\Delta G^\ddagger$  for benzene C–H activation from TpRu(L)(C<sub>6</sub>H<sub>6</sub>)Ph are 15.5 kcal/mol (L = CO) < 16.8 kcal/mol {L = P(OCH<sub>2</sub>)<sub>3</sub>CEt} < 17.1 kcal/mol (L = PMe<sub>3</sub>) < 21.7 kcal/mol {L = P(pyr)<sub>3</sub>}. Disregarding the bulky P(pyr)<sub>3</sub> system, DFT calculations suggest that benzene C–H activation is accelerated by less donating ligands, which contrasts the experimental results; however, experimental results are for the multistep

**SCHEME 10.** Proposed Catalytic Cycle for Olefin Hydroarylation<sup>a</sup>

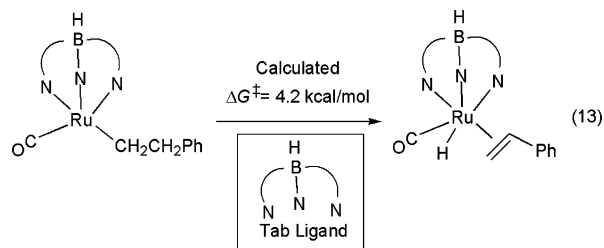
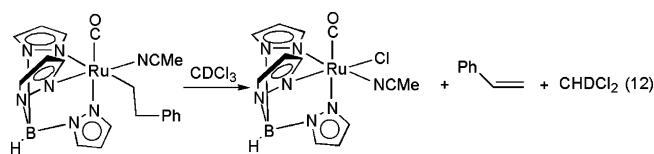
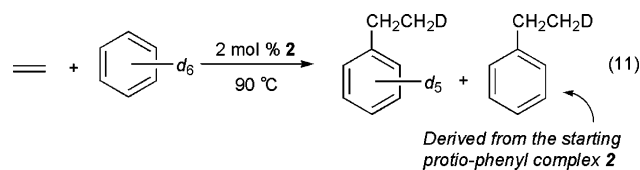
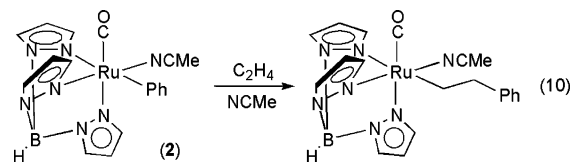
<sup>a</sup> Benzene and ethylene shown.

overall benzene C–H activation and render a direct comparison between calculation and experiment (even for the overall multistep process) difficult. Perhaps the most salient point from studies of stoichiometric benzene C–H activation by TpRu(L)(NCMe)Ph is that variation of L alters the energetics, but not substantially. The  $\Delta G^\ddagger$ s derived from experimental  $k_{\text{obs}}$  are within a 1 kcal/mol range, and calculated  $\Delta G^\ddagger$ s for benzene C–H activation vary by  $\sim 2$  kcal/mol if bulky P(pyr)<sub>3</sub> is excluded from consideration (Scheme 5).

#### 4. Catalytic Olefin Hydroarylation using TpRu(CO)(NCMe)Ph

TpRu(CO)(NCMe)Ph (**2**) is a precatalyst for olefin hydroarylation via a non-Friedel–Crafts pathway.<sup>7,16</sup> A proposed cycle based on experimental and computational studies is shown in Scheme 10 with typical catalytic results in Table 6.<sup>7,22</sup> The first step involves acetonitrile dissociation followed by olefin coordination to produce TpRu(CO)( $\eta^2$ -ethylene)Ph. Subsequent olefin insertion into the Ru–Ph bond results in C–C bond formation. Reacting TpRu(CO)(NCMe)Ph with ethylene in acetonitrile results in formation of TpRu(CO)(NCMe)(CH<sub>2</sub>CH<sub>2</sub>Ph),<sup>7</sup> which substantiates the suggestion that the TpRu(L)R systems can coordinate and insert olefins (eq 10). Furthermore, TpRu(CO)(NCMe)(CH<sub>2</sub>CH<sub>2</sub>Ph) reacts with C<sub>6</sub>D<sub>6</sub> to produce PhCH<sub>2</sub>CH<sub>2</sub>D and TpRu(CO)(NCMe)(Ph-*d*<sub>5</sub>), and catalysis with C<sub>6</sub>D<sub>6</sub> and C<sub>2</sub>H<sub>4</sub> yields C<sub>6</sub>D<sub>5</sub>CH<sub>2</sub>CH<sub>2</sub>D and C<sub>6</sub>H<sub>5</sub>CH<sub>2</sub>CH<sub>2</sub>D (the latter is derived from the starting protio-phenyl complex) as indicated by <sup>1</sup>H NMR and mass spectrometry (eq 11). Heating TpRu(CO)(NCMe)(CH<sub>2</sub>CH<sub>2</sub>Ph) in benzene (90 °C, 25 psi C<sub>2</sub>H<sub>4</sub>) produces TpRu(CO)(CH<sub>2</sub>CH<sub>2</sub>Ph)( $\eta^2$ -C<sub>2</sub>H<sub>4</sub>), the catalyst rest-

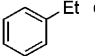
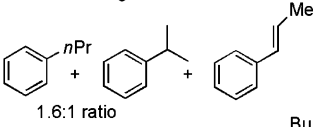
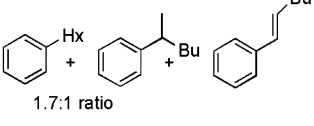
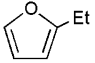
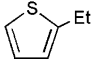
ing state, and ethylbenzene. The rate of catalytic ethylene hydrophenylation decreases with increasing ethylene pressure (Figure 4), consistent with TpRu(CO)( $\eta^2$ -ethylene)-(CH<sub>2</sub>CH<sub>2</sub>Ph) as the resting state. The final steps of the proposed catalytic cycle are ethylene/benzene exchange followed by Ru-mediated C–H activation of coordinated benzene to release ethylbenzene. Monitoring a CDCl<sub>3</sub> solution of TpRu(CO)(NCMe)(CH<sub>2</sub>CH<sub>2</sub>Ph) by <sup>1</sup>H NMR (70 °C) reveals the quantitative production of styrene, CHDCl<sub>2</sub>, and TpRu(CO)(NCMe)Cl (eq 12), which suggests that  $\beta$ -hydride elimination from TpRu(CO)(NCMe)(CH<sub>2</sub>CH<sub>2</sub>Ph) is kinetically facile. Consistent with the experimental results, DFT calculations on a (Tab)Ru(CO)(CH<sub>2</sub>CH<sub>2</sub>Ph) model reveal an activation barrier to  $\beta$ -hydride elimination of only 4.2 kcal/mol (eq 13). Thus, lack of styrene under catalytic conditions is best explained by reversible  $\beta$ -hydride elimination. Intermolecular kinetic isotope effects, as determined by catalysis in a 1:1 molar mixture of C<sub>6</sub>H<sub>6</sub> and C<sub>6</sub>D<sub>6</sub>, suggest that benzene C–H activation is the rate-determining step in the catalytic cycle, in agreement with DFT calculations of all steps in ethylene hydrophenylation by all TpRu(L)(NCMe)Ph catalyst precursors (Scheme 11).



#### 5. Comparison of Catalysis by TpRu(L)(NCMe)R Systems

We sought to probe the impact of L on TpRu(L)(NCMe)Ph catalysts by testing L = CO, PMe<sub>3</sub>, P(OCH<sub>2</sub>)<sub>3</sub>CeT, and P(pyr)<sub>3</sub> for

TABLE 6. Catalytic Addition of Arene C–H Bonds across C=C<sup>h</sup>

Arene	Unsaturated Substrate	TON	TOF <sup>a</sup>	Products
benzene	ethylene	51 (77) <sup>b</sup>	3.5 × 10 <sup>-3</sup>	
benzene	propylene	10	6.9 × 10 <sup>-4</sup>	
benzene	1-hexene <sup>d</sup>	11	5.0 × 10 <sup>-4</sup>	
furan <sup>e</sup>	ethylene	17 <sup>f</sup>	2.0 × 10 <sup>-4</sup>	
thiophene	ethylene	3 <sup>g</sup>	6.9 × 10 <sup>-5</sup>	

<sup>a</sup> Given as (mol **2**)<sup>-1</sup> s<sup>-1</sup>. <sup>b</sup> Turnovers observed after 24 h are given in parentheses. <sup>c</sup> Trace quantities of 1,3- and 1,4-diethylbenzene are also produced. <sup>d</sup> Fifty equivalents based on **2**, after 6 h. <sup>e</sup> Conditions of 120 °C, 40 psi, 1 mol % catalyst. <sup>f</sup> Twenty-four hours. <sup>g</sup> Three hours. <sup>h</sup> Unless otherwise noted, reaction conditions are 90 °C, 25 psi of gas, 0.1 mol% of **2**, 4 h.

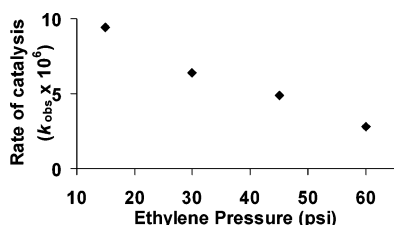
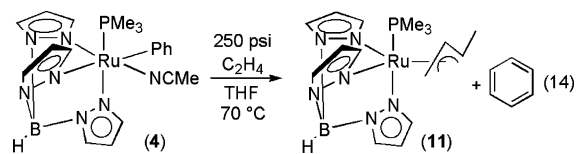


FIGURE 4. Dependence of the rate on ethylene pressure for addition of benzene to ethylene (0.1 mol % of **2**, 70 °C).

ethylene hydrophenylation. If the RDS of ethylene hydrophenylation is benzene C–H activation to form ethylbenzene, incorporation of PMe<sub>3</sub> or P(OCH<sub>2</sub>)<sub>3</sub>CEt is expected to accelerate ethylbenzene formation. However, as detailed below, catalysis with L = PMe<sub>3</sub> and P(OCH<sub>2</sub>)<sub>3</sub>CEt is hindered by a reduced rate of olefin insertion, which opens the door to competitive olefin C–H activation for **4** and **8**. The P(pyr)<sub>3</sub> complex **6** is a poor olefin hydroarylation catalyst due to the bulk of P(pyr)<sub>3</sub>, which prevents olefin coordination.

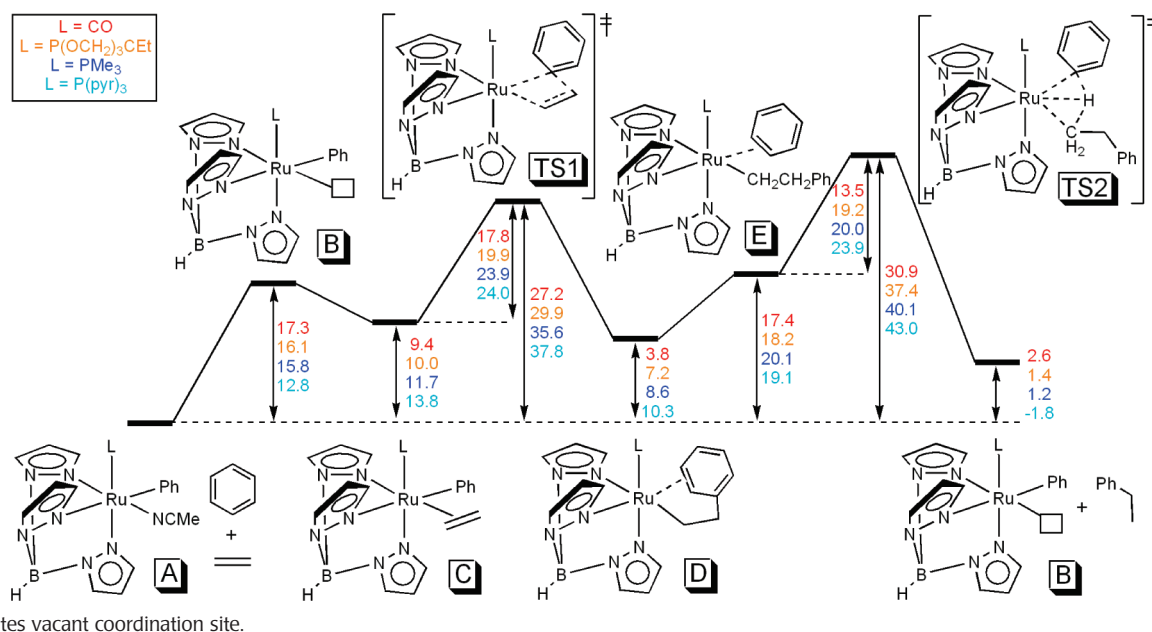
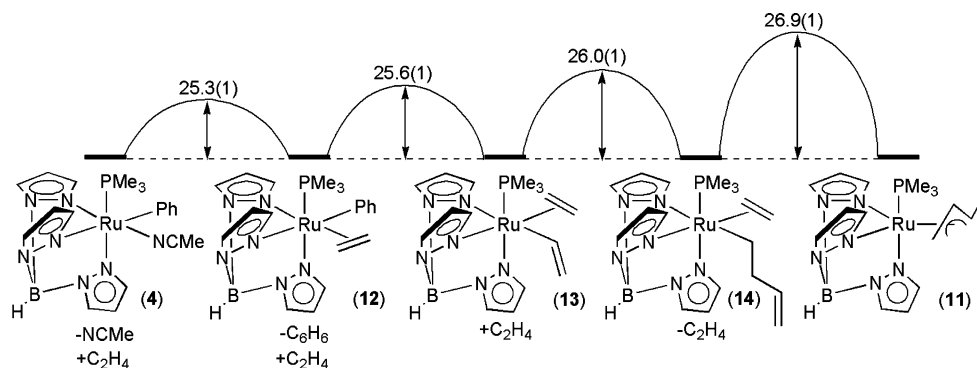
With **4** as catalyst (0.1 mol %) with benzene and ethylene, analysis of the catalyst mixture after heating reveals minimal production of ethylbenzene and near quantitative production of the η<sup>3</sup>-allyl complex TpRu(PMe<sub>3</sub>)(η<sup>3</sup>-C<sub>3</sub>H<sub>4</sub>Me) (**11**, eq 14), which was independently prepared. Monitoring the reaction of **4** with ethylene (80 psi) in THF-*d*<sub>8</sub> at 60 °C reveals that initial ethylene C–H activation is the culprit in the formation of **11** (Scheme 12). During the conversion, the emergence and disappearance of three primary Ru intermediates, TpRu(PMe<sub>3</sub>)(η<sup>2</sup>-C<sub>2</sub>H<sub>4</sub>)Ph (**12**), TpRu(PMe<sub>3</sub>)(η<sup>2</sup>-C<sub>2</sub>H<sub>4</sub>)(η<sup>1</sup>-C<sub>2</sub>H<sub>3</sub>) (**13**) (in addition to free benzene), and TpRu(PMe<sub>3</sub>)(η<sup>2</sup>-C<sub>2</sub>H<sub>4</sub>)(CH<sub>2</sub>CH<sub>2</sub>CH=CH<sub>2</sub>) (**14**), were observed.<sup>22</sup> Assuming that ethylene coordination to

TpRu(PMe<sub>3</sub>)(η<sup>1</sup>-C<sub>2</sub>H<sub>3</sub>) is rapid, conversion of **12** to **13** provides the rate of Ru-mediated ethylene C–H activation ( $k_{C_2H_4act} = 1.1(1) \times 10^{-4} s^{-1}$ ). Ethylene insertion into the Ru–vinyl bond to form **14** occurs with  $k_{C_2H_4ins} = 5.9(6) \times 10^{-5} s^{-1}$ . Thus, we propose that the poor catalytic activity exhibited by **4** is due to a substantial ΔG<sup>‡</sup> for ethylene insertion that allows ethylene C–H activation to compete and results in a relatively rapid removal of active catalyst via formation of the η<sup>3</sup>-allyl complex **11**. DFT calculations (Scheme 11) suggest that replacing CO with PMe<sub>3</sub> increases the activation barrier for ethylene coordination and insertion with ΔΔG<sup>‡</sup> = 9.9 kcal/mol (Table 7).



Similar to the PMe<sub>3</sub> complex **4**, at 250 psi ethylene in THF at 70 °C complex **2** is cleanly converted to TpRu(CO)(η<sup>3</sup>-C<sub>3</sub>H<sub>4</sub>Me) (**16**) in 98% yield. However, monitoring the conversion of **2** and ethylene (80 psi) to **16** at 60 °C in THF-*d*<sub>8</sub> reveals important differences from the PMe<sub>3</sub> complex **4** (Scheme 13). The reaction of **2** with ethylene (in the absence of benzene) proceeds via ethylene coordination and rapid olefin insertion followed by ethylene C–H activation to produce free ethylbenzene and presumably TpRu(CO)(η<sup>2</sup>-C<sub>2</sub>H<sub>4</sub>)(η<sup>1</sup>-C<sub>2</sub>H<sub>3</sub>). As opposed to **4** (see above), a more rapid rate of olefin insertion for the CO system **2** is indicated since neither TpRu(CO)(η<sup>2</sup>-C<sub>2</sub>H<sub>4</sub>)(Ph) nor TpRu(CO)(η<sup>2</sup>-C<sub>2</sub>H<sub>4</sub>)(η<sup>1</sup>-C<sub>2</sub>H<sub>3</sub>) is



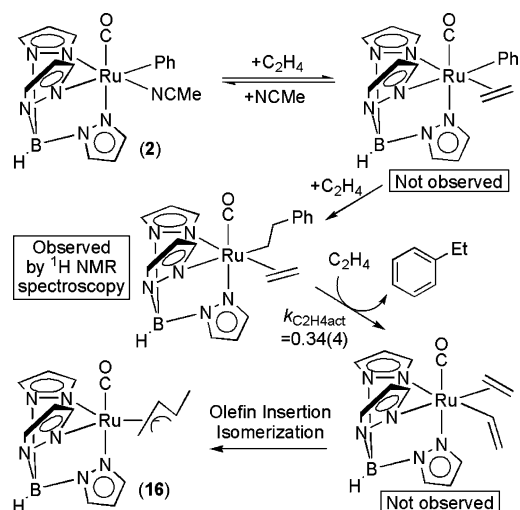
**SCHEME 11.** Calculated Free Energies (kcal/mol) for Catalytic Cycle of Ethylene Hydrophenylation by TpRu(L)(NCMe)Ph (L = CO, P(MeO)<sub>2</sub>CEt, or P(pyr)<sub>3</sub>)<sup>a</sup>**SCHEME 12.** Proposed Mechanism for Formation of TpRu(PMe<sub>3</sub>)(η<sup>3</sup>-C<sub>3</sub>H<sub>4</sub>Me) (11) from the Reaction of TpRu(PMe<sub>3</sub>)(NCMe)Ph (4) and Ethylene<sup>a</sup>**TABLE 7.** Combined Steric and Electronic Impact on the Ethylene Coordination/Insertion Step for Olefin Hydroarylation by TpRu(L)(NCMe)Ph<sup>a</sup>

complex	L	ΔG (kcal/mol) for B → TS1
<b>2</b>	CO	9.9
<b>8</b>	P(OCH <sub>2</sub> ) <sub>3</sub> CEt	13.8
<b>4</b>	PMe <sub>3</sub>	19.8
<b>6</b>	P(pyr) <sub>3</sub>	25.0

<sup>a</sup> B in the table refers to species B in Scheme 11.

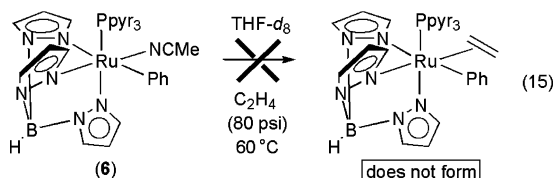
observed by <sup>1</sup>H NMR spectroscopy. The rate of ethylene C–H activation by TpRu(CO)(η<sup>2</sup>-C<sub>2</sub>H<sub>4</sub>)(CH<sub>2</sub>CH<sub>2</sub>Ph) is  $k_{C_2H_4act} = 3.4(4) \times 10^{-5} s^{-1}$ , ~3 times slower than ethylene C–H activation by the PMe<sub>3</sub> system. Thus, the relative rates of olefin C–H activation are similar to relative rates of overall benzene C–H(D) activation (Table 4).

Combined experimental and computational studies suggest that the major impact of replacing CO with PMe<sub>3</sub> is to increase the activation barrier to ethylene insertion, which results in kinetically competitive ethylene C–H activation. Inhibition of olefin coordination and insertion may result from enhanced Ru-to-olefin dπ-to-π\* backbonding in C (Scheme 11) as Ru electron density is increased. Consistent with this suggestion, for L = CO, P(OCH<sub>2</sub>)<sub>3</sub>CEt, or PMe<sub>3</sub>, calculated ΔG<sup>‡</sup> values for ethylene insertion (17.8, 19.9, and 23.9 kcal/mol, respectively) increase with increasing donor ability of L (Scheme 11). Perhaps more instructive are calculated ΔG<sup>‡</sup> values for conversion of 16-electron TpRu(L)Ph (B) to TS1. The data (Table 7) reflect the combined impact of sterics and electronics with olefin coordination/insertion favored by small (e.g., CO) and less donating ligands. It is notable that the two

**SCHEME 13.** Proposed Mechanism for Formation of TpRu(CO)( $\eta^3$ -C<sub>3</sub>H<sub>4</sub>Me) (**16**)<sup>a</sup><sup>a</sup> Rate constant reported in units of 10<sup>-4</sup> s<sup>-1</sup>.

least efficient catalysts, L = PMe<sub>3</sub> or P(pyr)<sub>3</sub>, are calculated to have the most substantial  $\Delta G$  for conversion of B to TS1.

Having observed that strongly donating PMe<sub>3</sub> inhibits olefin insertion, we moved to the tris-*N*-pyrrolylphosphine {P(pyr)<sub>3</sub>} ligand with similar  $\pi$ -acidity as CO yet with more steric bulk than CO and PMe<sub>3</sub>. Under most conditions, the P(pyr)<sub>3</sub> complex **6** does not perform catalytic olefin hydroarylation. An X-ray diffraction study of **6** illustrates the impact of the bulky P(pyr)<sub>3</sub> ligand with close proximity between P(pyr)<sub>3</sub> and phenyl ligands (Figure 5). Heating **6** (60 °C, 80 psi ethylene) in THF-*d*<sub>8</sub> for 5.5 days does not reveal the formation of TpRu{P(pyr)<sub>3</sub>}( $\eta^2$ -C<sub>2</sub>H<sub>4</sub>)Ph (eq 15), whereas TpRu(L)( $\eta^2$ -C<sub>2</sub>H<sub>4</sub>)Ph (L = CO or PMe<sub>3</sub>) is readily produced under these conditions. The bulky P(pyr)<sub>3</sub> likely inhibits ethylene coordination to form TpRu{P(pyr)<sub>3</sub>}( $\eta^2$ -C<sub>2</sub>H<sub>4</sub>)Ph. Calculations reveal energetics consistent with this proposal. Calculated  $\Delta G$  for coordination of ethylene to TpRu(L)(Ph) is negative for L = PMe<sub>3</sub> (-4.1 kcal/mol), P(OCH<sub>2</sub>)<sub>3</sub>CEt (-6.1 kcal/mol), and CO (-7.9 kcal/mol), but for L = P(pyr)<sub>3</sub> the coordination of ethylene is calculated to be endergonic with  $\Delta G = +1.0$  kcal/mol (Scheme 11).<sup>23</sup>



Based on the aforementioned results, the reduced cone angle (101°) of the bicyclic phosphite ligand P(OCH<sub>2</sub>)<sub>3</sub>CEt was anticipated to allow olefin coordination while the moderate  $\pi$ -acidity was expected to facilitate olefin insertion relative to the PMe<sub>3</sub> system. In contrast to the P(pyr)<sub>3</sub> system, DFT calcu-

lations suggest that ethylene coordination by TpRu{P(OCH<sub>2</sub>)<sub>3</sub>CEt}Ph is favorable (Scheme 11) and that conversion of TpRu{P(OCH<sub>2</sub>)<sub>3</sub>CEt}Ph to the olefin insertion transition state is favored over the PMe<sub>3</sub> complex by 6 kcal/mol (Table 7).<sup>26</sup> Indeed, heating TpRu{P(OCH<sub>2</sub>)<sub>3</sub>CEt}(NCMe)Ph (**8**) in benzene under moderate ethylene pressure results in production of ethylbenzene with TON = 10 after 28 h at 90 °C.<sup>26</sup> However, catalysis is ultimately halted by formation of TpRu{P(OCH<sub>2</sub>)<sub>3</sub>CEt}( $\eta^3$ -C<sub>3</sub>H<sub>4</sub>Me) (Scheme 14). Although ethylene insertion is sufficiently facile to compete with ethylene C-H activation, ultimately catalyst decomposition occurs via the latter reaction.

The amalgam of studies for TpRu(L)Ph suggests that the key crossroads in the catalysis occurs after formation of TpRu(L)( $\eta^2$ -C<sub>2</sub>H<sub>4</sub>)Ph. The reaction coordinates were calculated for olefin C-H activation from  $\eta^2$ -C<sub>2</sub>H<sub>4</sub> complexes **C** for L = CO, P(OCH<sub>2</sub>)<sub>3</sub>CEt, and PMe<sub>3</sub> (Scheme 15). The ethylene C-H activation event passes through an OHM transition state (TS3) to form a Ru-vinyl intermediate **F**. Calculated activation free energies relative to **C** for the ethylene C-H activation step are higher than those of the ethylene insertion step. Table 8 displays relevant energetic parameters. From this point, for successful catalysis olefin insertion and subsequent benzene coordination/C-H activation must be substantially more rapid than olefin C-H activation. Hence, the  $\Delta\Delta G^\ddagger$  shown in the fourth column of Table 8 should be optimized. Consistent with experimental observations (see above), L = PMe<sub>3</sub> has the smallest  $\Delta\Delta G^\ddagger$ , which should result in olefin C-H activation competing with olefin insertion. The corresponding calculated  $\Delta\Delta G^\ddagger$  values for CO and P(OCH<sub>2</sub>)<sub>3</sub>CEt systems suggest that both of these systems should favor olefin insertion to a greater extent than the PMe<sub>3</sub> system, which is observed experimentally. However, the phosphite system only gives a few turnovers of ethylbenzene prior to olefin C-H activation and formation of  $\eta^3$ -allyl. Following olefin insertion, the catalysts coordinate benzene and initiate C-H activation to complete the catalytic cycle. Alternatively, olefin deinsertion reverts the system to TpRu(L)( $\eta^2$ -C<sub>2</sub>H<sub>4</sub>)Ph and provides another opportunity for competitive olefin C-H activation. Comparing calculated  $\Delta\Delta G^\ddagger$  values for (a) benzene coordination and subsequent C-H activation (i.e., benzene C-H activation starting from TpRu(L)CH<sub>2</sub>CH<sub>2</sub>Ph) and (b) deinsertion from TpRu(L)CH<sub>2</sub>CH<sub>2</sub>Ph provides insight into aptitude for these two processes (Table 8, last column). Clearly, the CO complex, with a calculated  $\Delta\Delta G^\ddagger$  of 3.7 kcal/mol, is predicted to have a greater predilection toward benzene coordination and C-H activation than the phosphite system with a calculated  $\Delta\Delta G^\ddagger = 7.5$  kcal/mol.

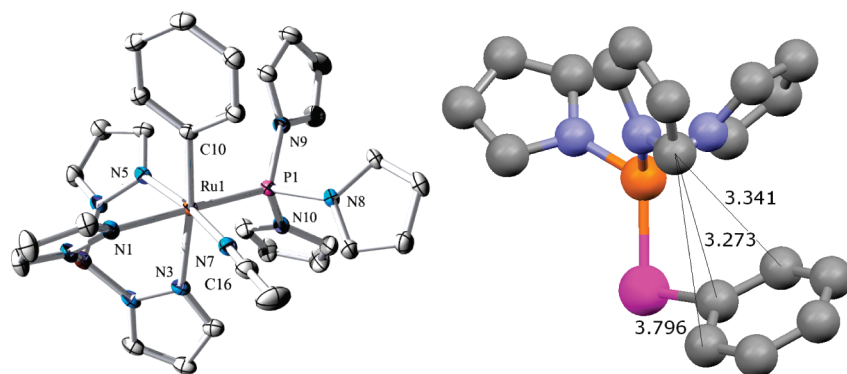
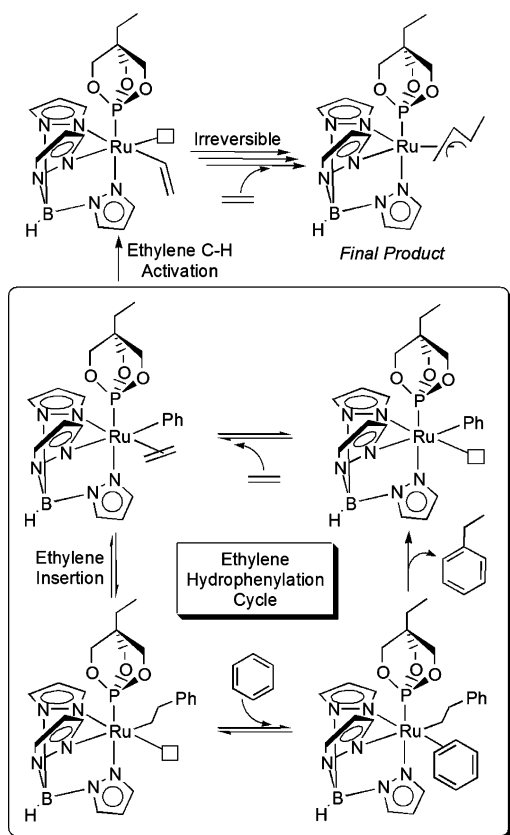


**FIGURE 5.** ORTEP of  $\text{TpRu}\{\text{P}(\text{pyr})_3\}(\text{NCMe})$  (**6**) (left) and ball and stick diagram (right) of  $\text{Ru}\{\text{P}(\text{pyr})_3\}\text{Ph}$  fragment with distances (Å) from nearest pyrrolyl 2-position carbon to ipso and meta carbons of phenyl ring (hydrogen atoms omitted).

**SCHEME 14.** Competition between Ethylene Insertion, Which Leads to Ethylene Hydrophenylation, and Ethylene C–H Activation, Which Leads to Irreversible Formation of  $\text{TpRu}\{\text{P}(\text{OCH}_2)_3\text{Cet}\}(\eta^3\text{-C}_3\text{H}_4\text{Me})$



**SCHEME 15.** Comparison of Calculated Gibbs Free Energies (kcal/mol) for Ethylene Insertion and Ethylene C–H Activation by  $\text{TpRu}(\text{L})(\text{NCMe})\text{Ph}$  {L = CO,  $\text{P}(\text{OCH}_2)_3\text{Cet}$  and  $\text{PMe}_3$ }

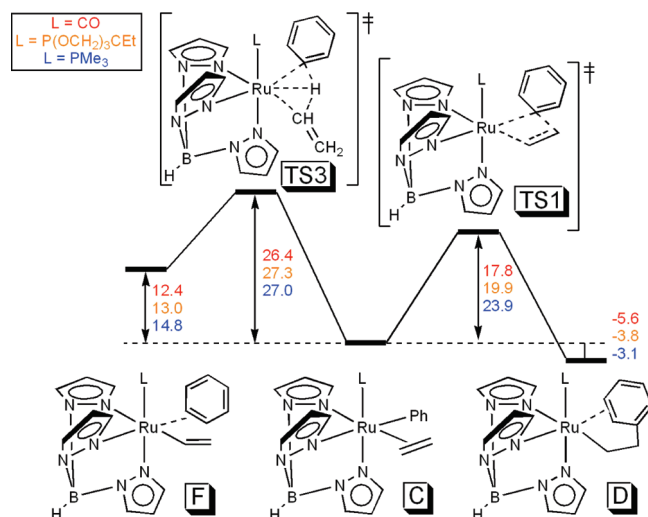


**TABLE 8.** Calculations Relevant to Olefin Hydroarylation Catalyzed by  $\text{TpRu}(\text{L})\text{Ph}$  (kcal/mol at 298 K)

L	$\Delta G^\ddagger$ $\text{C}_2\text{H}_4\text{C-H}$ activation <sup>a</sup>	$\Delta G^\ddagger$ $\text{C}_2\text{H}_4$ insertion <sup>a</sup>	$\Delta\Delta G^{\ddagger b}$	$\Delta G^\ddagger$ $\text{C}_6\text{H}_6$ activation <sup>c</sup>	$\Delta G^\ddagger$ deinsertion <sup>d</sup>	$\Delta\Delta G^{\ddagger e}$
CO	26.4	17.8	8.6	27.1	23.4	3.7
$\text{P}(\text{OCH}_2)_3\text{Cet}$	27.3	19.9	7.4	30.2	22.7	7.5
$\text{PMe}_3$	27.0	23.9	3.1	31.5	27.0	4.5

<sup>a</sup> From  $\text{TpRu}(\text{L})(\eta^2\text{-C}_2\text{H}_4)\text{Ph}$ . <sup>b</sup>  $\Delta G^\ddagger(\text{C-H activation}) - \Delta G^\ddagger(\text{insertion})$ . <sup>c</sup> Calculated  $\Delta G^\ddagger$  values for benzene coordination and C–H activation after olefin insertion step (from complexes D in Scheme 14). <sup>d</sup> Calculated  $\Delta G^\ddagger$  values for ethylene deinsertion. <sup>e</sup>  $\Delta G^\ddagger(\text{benzene C-H activation}) - \Delta G^\ddagger(\text{deinsertion})$ .

## 6. Summary/Future Catalyst Design

Through combined experimental and computational studies, we have methodically probed the impact of steric and electronic properties of ancillary ligands on olefin hydroarylation using octahedral Ru(II) catalysts. Using cyclic voltammetry to estimate metal-centered electron density, our studies of  $\text{TpRu}^{\text{II}}$  systems suggest that optimal catalysts will have  $d^6/d^5$  redox potentials of  $\sim 1.0$  V (versus NHE). We have not yet studied a system for which the Ru(III/II) potential is  $>1.0$  V and cannot

comment on the impact of reduced electron density relative to  $\text{TpRu}(\text{CO})(\text{NCMe})\text{Ph}$ . Our results suggest that increasing the bulk of L beyond the steric profile of CO can increase linear/branched ratios for hydroarylation of  $\alpha$ -olefins,<sup>7</sup> but this strategy should be implemented with cognizance of the limits on steric profile of L (see below). Perhaps most importantly within the realm of rational homogeneous catalyst design, the integration of theory and experiment to yield detailed information about the kinetics and thermodynamics of various

reactions (and side reactions) that characterize a catalytic cycle, starting from a  $\text{TpRu}(\text{CO})(\text{NCMe})\text{Ph}$ , suggests attractive targets for future catalysts:

- (1) Replacing CO of  $\text{TpRu}(\text{CO})(\text{NCMe})\text{Ph}$  with ligands that have similar  $\pi$ -acidic properties but increased steric profile may provide selective catalysts for transformations of  $\alpha$ -olefins. However, in combination with the Tp ligand, ligands with cone angles  $>145^\circ$  will likely inhibit olefin coordination. For  $\text{TpRu}(\text{L})$  systems, and possibly for closely related systems, the desired size is larger than CO but smaller than  $\text{P}(\text{pyr})_3$ .
- (2) Since incorporation of strongly donating phosphine ligands (e.g.,  $\text{PMe}_3$ ) for  $\text{TpRu}(\text{L})(\text{NCMe})\text{Ph}$  systems is limited by the impact on  $\Delta G^\ddagger$  for olefin insertion, replacing the Tp ligand with tris-nitrogen chelates that are charge neutral is an attractive target. This will allow incorporation of more donating ligands L (in place of CO) and thus permit greater steric modulation without substantial increase in Ru-based electron density.
- (3) Similar to the use of charge neutral nitrogen chelates, replacing Ru of  $\text{TpRu}(\text{L})(\text{NCMe})\text{Ph}$  with less electron-rich metals should allow incorporation of more donating ligands L (relative to CO) and greater variability in the steric profile. It will be interesting to learn whether the relative energetics for key steps inside and outside the catalytic cycle will exhibit a similar dependence on L as the ligand framework is retained but the identity of the metal is altered.
- (4) Moving away from the octahedral and  $d^6$  motif for catalyst precursors may provide catalytic systems that vary dramatically from the  $\text{TpRu}(\text{L})\text{R}$  structure in terms of relative energetics of key steps. Thus, alternative avenues to enhance activity and control selectivity might be available outside an octahedral  $d^6$  paradigm. For example, in unpublished work we are pursuing chemistry of Ru(II) systems in low-coordination environments, and we and others have recently reported Pt(II) catalyst precursors that give promising initial results for olefin hydroarylation using unactivated substrates.<sup>12–14</sup>

*T.B.G. acknowledges the Department of Energy (DOE-BES; Grant DE-FG02-03ER15490) and the primary collaborators: Jeffrey L. Petersen, Paul D. Boyle, Laurel A. Goj, John P. Lee, Marty Lail, Karl A. Pittard, Nicholas Foley, and Kimberly C. Riley. T.R.C. acknowledges DOE-BES (Grant No. DE-FG02-03ER15387), the Department of Education for support of CASCaM, the NSF (Grants CHE-0342824 and CHE-0741936) for facilities, and Khaldoon A. Barakat and Aaron W. Pierpont. Z.K. acknowledges the State Scholarship Fund of CSC (Grant No.*

*2007102840) and the NSF-sponsored Center for Enabling New Technologies through Catalysis (CENTC; Grant CHE-0650456).*

## BIOGRAPHICAL INFORMATION

**Nicholas A. Foley** received a B.S. in Biochemistry from the University of North Carolina at Chapel Hill and is currently pursuing a Ph. D. degree at North Carolina State University.

**John P. Lee** obtained a B.S. in Chemistry from the University of Tennessee at Chattanooga where he worked with Gregory J. Grant and obtained a Ph.D. from North Carolina State University in 2008 under the direction of Gunnoe. He is currently a research chemist at Eastman Chemical.

**Zhuofeng Ke** earned his B.Sc. (Chemistry) and M.Sc. (Polymer Chemistry and Physics with Qing Wu) at Sun Yat-sen University. He has been working toward his Ph.D. in computational chemistry (with Cunyuan Zhao) applied to catalysis. In 2007, he received a scholarship from the State Scholarship Fund of China to work with Wes Borden and Tom Cundari at UNT/CASCaM.

**T. Brent Gunnoe** obtained a B.A. in Chemistry from West Virginia University where he performed research with Jeffrey L. Petersen, obtained his Ph. D. from the University of North Carolina under the direction of Joseph L. Templeton, and worked as a postdoctoral associate with W. Dean Harman at the University of Virginia. He began his independent career at North Carolina State University in 1999 and moved to the University of Virginia in 2008. Research in the Gunnoe group is focused on studies of inorganic and organometallic complexes including homogeneous catalysis applications.

**Thomas R. Cundari** obtained a B.S. in Chemistry at Pace University. After completing his Ph.D. at the University of Florida with Russ Drago, he spent a postdoctoral year at North Dakota State University with Mark Gordon. He joined the faculty of the University of Memphis in 1991. In 2002, he moved to UNT, having recently (2008) been promoted to Regents Professor. Research in the Cundari group is focused on modeling metals in catalysis and materials chemistry with emphasis on integration of theory and experiment.

## FOOTNOTES

\*To whom correspondence should be addressed. E-mail addresses: tbg7h@virginia.edu; t@unt.edu.

## REFERENCES

- 1 Labinger, J. A.; Bercaw, J. E. Understanding and Exploiting C-H Bond Activation. *Nature* **2002**, *417*, 507–514.
- 2 Goldberg, K. I.; Goldman, A. S., Eds. *Activation and Functionalization of C-H Bonds*; ACS Symposium Series 885; American Chemical Society: Washington, DC, 2004.
- 3 Shilov, A. E.; Shul'pin, G. B. *Activation and Catalytic Reactions of Saturated Hydrocarbons in the Presence of Metal Complexes*; Kluwer Academic Publishers: Dordrecht, The Netherlands, 2000; Vol. 21.
- 4 Ritleng, V.; Sirlin, C.; Pfeffer, M. Ru-, Rh-, and Pd-Catalyzed C-C Bond Formation Involving C-H Activation and Addition on Unsaturated Substrates: Reactions and Mechanistic Aspects. *Chem. Rev.* **2002**, *102*, 1731–1769.
- 5 Goj, L. A.; Gunnoe, T. B. Developments in Catalytic Aromatic C-H Transformations: Promising Tools for Organic Synthesis. *Curr. Org. Chem.* **2005**, *9*, 671–685.
- 6 Olah, G. A.; Molnár, Á. *Hydrocarbon Chemistry*, 2nd ed.; Wiley-Interscience: New York, 2003; pp 229–232.

- 7 Lail, M.; Bell, C. M.; Conner, D.; Cundari, T. R.; Gunnoe, T. B.; Petersen, J. L. Experimental and Computational Studies of Ru(II) Catalyzed Addition of Arene C—H Bonds to Olefins. *Organometallics* **2004**, *23*, 5007–5020.
- 8 Wittcoff, H. A.; Reuben, B. G.; Plotkin, J. S. *Industrial Organic Chemicals*, 2nd ed.; Wiley-Interscience: Hoboken, NJ, 2004; pp 553–558.
- 9 Olah, G. A.; Molnár, Á. *Hydrocarbon Chemistry*, 2nd ed.; Wiley-Interscience: New York, 2003; pp 262–267.
- 10 Hassan, J.; Sévignon, M.; Gozzi, C.; Schulz, E.; Lemaire, M. Aryl—Aryl Bond Formation One Century after the Discovery of the Ullmann Reaction. *Chem. Rev.* **2002**, *102*, 1359–1470.
- 11 Miyauro, N.; Suzuki, A. Palladium-Catalyzed Cross-Coupling Reactions of Organoboron Compounds. *Chem. Rev.* **1995**, *95*, 2457–2483.
- 12 Luedtke, A. T.; Goldberg, K. I. Intermolecular Hydroarylation of Unactivated Olefins Catalyzed by Homogeneous Platinum Complexes. *Angew. Chem., Int. Ed.* **2008**, *47*, 7694–7696.
- 13 McKeown, B. A.; Foley, N. A.; Lee, J. P.; Gunnoe, T. B. Hydroarylation of Unactivated Olefins Catalyzed by Platinum(II) Complexes. *Organometallics* **2008**, *27*, 4031–4033.
- 14 Karshedt, D.; Bell, A. T.; Tilley, T. D. Pt—Ag Catalyst System for Hydroarylations with Unactivated Arenes and Olefins. *Organometallics* **2004**, *23*, 4169–4171.
- 15 Matsumoto, T.; Periana, R. A.; Taube, D. J.; Yoshida, H. Regioselective Hydrophenylation of Olefins Catalyzed by an Ir(III) Complex. *J. Mol. Catal. A: Chem.* **2002**, *180*, 1–18.
- 16 Lail, M.; Arrowood, B. N.; Gunnoe, T. B. Addition of Arenes to Ethylene and Propene Catalyzed by Ruthenium. *J. Am. Chem. Soc.* **2003**, *125*, 7506–7507.
- 17 Pittard, K. A.; Lee, J. P.; Cundari, T. R.; Gunnoe, T. B.; Petersen, J. L. Reactions of TpRu(CO)(NCMe)(Me) (Tp = Hydridotris(pyrazolyl)borate) with Heteroaromatic Substrates: Stoichiometric and Catalytic C—H Activation. *Organometallics* **2004**, *23*, 5514–5523.
- 18 Arrowood, B. N.; Lail, M.; Gunnoe, T. B.; Boyle, P. D. Radical Polymerization of Styrene and Methyl Methacrylate with Ruthenium(II) Complexes. *Organometallics* **2003**, *22*, 4692–4698.
- 19 Lail, M.; Gunnoe, T. B.; Barakat, K. A.; Cundari, T. R. Conversions of Ruthenium(III) Alkyl Complexes to Ruthenium(II) through Ru—C<sub>alkyl</sub> Bond Homolysis. *Organometallics* **2005**, *24*, 1301–1305.
- 20 Pittard, K. A.; Cundari, T. R.; Gunnoe, T. B.; Day, C. S.; Petersen, J. L. Ruthenium(II)-Mediated Carbon—Carbon Bond Formation between Acetonitrile and Pyrrole: Combined Experimental and Computational Study. *Organometallics* **2005**, *24*, 5015–5024.
- 21 Goj, L. A.; Lail, M.; Pittard, K. A.; Riley, K. C.; Gunnoe, T. B.; Petersen, J. L. Reactions of TpRu(CO)(NCMe)(Ph) with Electron-rich Olefins: Examples of Stoichiometric C—S, C—O and C—H Bond Cleavage. *Chem. Commun.* **2006**, 982–984.
- 22 Foley, N. A.; Lail, M.; Lee, J. P.; Gunnoe, T. B.; Cundari, T. R.; Petersen, J. L. Comparative Reactivity of TpRu(L)(NCMe)Ph (L = CO or PMe<sub>3</sub>): Impact of Ancillary Ligand L on Activation of Carbon-Hydrogen Bonds Including Catalytic Hydroarylation and Hydrovinylation/Oligomerization of Ethylene. *J. Am. Chem. Soc.* **2007**, *129*, 6765–6781.
- 23 Foley, N. A.; Lail, M.; Gunnoe, T. B.; Cundari, T. R.; Boyle, P. D.; Petersen, J. L. Combined Experimental and Computational Study of TpRu[P(pyr)<sub>3</sub>](NCMe)Me (pyr = *N*-pyrrolyl): Inter- and Intramolecular Activation of C—H Bonds and the Impact of Sterics on Catalytic Hydroarylation of Olefins. *Organometallics* **2007**, *26*, 5507–5516.
- 24 Lee, J. P.; Jimenez-Halla, O. C.; Cundari, T. R.; Gunnoe, T. B. Reactivity of TpRu(L)(NCMe)R (L = CO, PMe<sub>3</sub>; R = Me, Ph) Systems with Isonitriles: Experimental and Computational Studies toward the Intra- and Intermolecular Hydroarylation of Isonitriles. *J. Organomet. Chem.* **2007**, *692*, 2175–2186.
- 25 Lee, J. P.; Pittard, K. A.; DeYonker, N. J.; Cundari, T. R.; Gunnoe, T. B.; Petersen, J. L. Reactions of a Ru(II) Phenyl Complex with Substrates that Possess C—N or C—O Multiple Bonds: C—C Bond Formation, N—H Bond Cleavage, and Decarbonylation Reactions. *Organometallics* **2006**, *25*, 1500–1510.
- 26 Foley, N. A.; Ke, Z.; Gunnoe, T. B.; Cundari, T. R.; Petersen, J. L. Aromatic C—H Activation and Catalytic Hydrophenylation of Ethylene by TpRu(P(OCH<sub>2</sub>)<sub>3</sub>CEt)(NCMe)Ph. *Organometallics* **2008**, *27*, 3007–3017.
- 27 Kakiuchi, F.; Chatani, N. Catalytic Methods for C—H Bond Functionalization: Application in Organic Synthesis. *Adv. Synth. Catal.* **2003**, *345*, 1077–1101.
- 28 Kakiuchi, F.; Murai, S. Catalytic C—H/Olefin Coupling. *Acc. Chem. Res.* **2002**, *35*, 826–834.
- 29 Tolman, C. A. Steric Effects of Phosphorus Ligands in Organometallic Chemistry and Homogeneous Catalysis. *Chem. Rev.* **1977**, *77*, 313–348.
- 30 Moloy, K. G.; Petersen, J. L. *N*-Pyrrolyl Phosphines: An Unexploited Class of Phosphine Ligands with Exceptional  $\pi$ -Acceptor Character. *J. Am. Chem. Soc.* **1995**, *117*, 7696–7710.
- 31 Huttemann, T. J.; Foxman, B. M.; Sperati, C. R.; Verkade, J. G. Transition Metal Complexes of a Constrained Phosphite Ester. IV. Compounds of Cobalt(I), Cobalt(III), Nickel(II), and Nickel(0). *Inorg. Chem.* **1965**, *4*, 950–953.
- 32 DeYonker, D. J.; Foley, N. A.; Cundari, T. R.; Gunnoe, T. B.; Petersen, J. L. Combined Experimental and Computational Studies on the Nature of Aromatic C—H Activation by Octahedral Ru(II) Complexes: Evidence for  $\sigma$ -Bond Metathesis from Hammett Studies. *Organometallics* **2007**, *26*, 6604–6611.
- 33 Feng, Y.; Lail, M.; Foley, N. A.; Gunnoe, T. B.; Barakat, K. A.; Cundari, T. R.; Petersen, J. L. Hydrogen—Deuterium Exchange between TpRu(PMe<sub>3</sub>)(L)X (L = PMe<sub>3</sub> and X = OH, OPh, Me, Ph, or NHPH; L = NCMe and X = Ph) and Deuterated Arene Solvents: Evidence for Metal-Mediated Processes. *J. Am. Chem. Soc.* **2006**, *128*, 7982–7994.
- 34 Lam, W. H.; Jia, G.; Lin, Z.; Lau, C. P.; Eisenstein, O. Theoretical Studies on the Metathesis Processes, [Tp(PH<sub>3</sub>)MR( $\eta^2$ -H-CH<sub>3</sub>)] - [Tp(PH<sub>3</sub>)M(CH<sub>3</sub>)( $\eta^2$ -H-R)] (M = Fe, Ru, and Os; R = H and CH<sub>3</sub>). *Chem. Eur. J.* **2003**, *9*, 2775–2782.
- 35 Bhalla, G.; Liu, X. Y.; Oxgaard, J.; Goddard, W. A., III; Periana, R. A. Synthesis, Structure, and Reactivity of O-Donor Ir(III) Complexes: C—H Activation Studies with Benzene. *J. Am. Chem. Soc.* **2005**, *127*, 11372–11389.
- 36 Vastine, B. A.; Hall, M. B. C—H Bond Activation: Two, Three, or More Mechanisms. *J. Am. Chem. Soc.* **2007**, *129*, 12068–12069.